Research Square

Preprints are preliminary reports that have not undergone peer review.
They should not be considered conclusive, used to inform clinical practice,
or referenced by the media as validated information.

Multi-omics analysis reveals PITX1 as a predictor of immunotherapy efficacy in clear cell renal cell carcinoma

Dingbang Liu
West China Hospital of Sichuan University
Junjie Zhao
West China Hospital of Sichuan University
Zilin Wang
West China Hospital of Sichuan University
Yanfeng Tang
West China Hospital of Sichuan University
Jiayu Liang
West China Hospital of Sichuan University
Hao Zeng
kucaizeng@163.com

West China Hospital of Sichuan University

Research Article

Keywords: PITX1, clear cell renal cell carcinoma, immunotherapy, tumor microenvironment

Posted Date: November 3rd, 2026

DOI: https://doi.org/10.21203/rs.3.rs-11049491/v1

License: This work is licensed under a Creative Commons Attribution 4.0 International License.
Read Full License

Additional Declarations: No competing interests reported.

Abstract

Background

Immune checkpoint inhibitors (ICIs) have improved outcomes in advanced clear cell renal cell carcinoma (ccRCC), but predictive biomarkers are lacking. The role of paired-like homeodomain 1 (PITX1) in ccRCC remains unclear.

Methods

Machine learning identified PITX1 as a key biomarker. Multi-omics analyses integrated bulk RNA-seq, single-cell RNA-seq (scRNA-seq), spatial transcriptomics (ST), data from three randomized controlled trials (IMmotion151, CheckMate025, JAVELIN Renal 101) and West China Hospital ccRCC cohort.

Results

PITX1 was upregulated in ccRCC, associated with BAP1 mutation and hypomethylation. scRNA-seq and ST revealed the expression patterns of PITX1 in different cell clusters. High PITX1 expression correlated with advanced clinicopathological features, poor survival, and metabolic reprogramming towards glucose and methionine metabolism. Enrichment analysis suggested high PITX1 would lead to more malignant tumor biological behaviors. It shaped an immunosuppressive microenvironment with regulatory T cells (Tregs) infiltrated and elevated immune checkpoints. Crucially, high PITX1 indicates inferior benefits for patients receiving immunotherapy.

Conclusion

PITX1 is a novel biomarker linked to aggressive tumor behavior, metabolic alteration, and immune evasion, predicting poor response to immunotherapy in ccRCC.

Introduction

Renal cell carcinoma (RCC), which comprises 80–90% of all malignant kidney tumors, represents a major clinical challenge within urologic oncology[1]. Clear cell RCC (ccRCC) is the most common histologic subtype and is characterized by substantial molecular heterogeneity driven by genomic and epigenomic alterations[2, 3]. Over the past twenty years, anti-angiogenic agents have become a standard first-line treatment for advanced ccRCC, considering the significant role of dysregulated angiogenesis in its pathogenesis. More recently, the treatment paradigm has undergone a transformative shift with the introduction of immune checkpoint inhibitors (ICIs). Several ICIs, including anti-programmed cell death protein 1 (PD-1) (e.g., nivolumab), anti-programmed cell death ligand 1 (PD-L1) (e.g., atezolizumab, avelumab), and anti-cytotoxic T lymphocyte-associated antigen-4 (CTLA-4) (e.g., ipilimumab) agents,

have been approved for advanced ccRCC, either as monotherapy or, more commonly, in combination with other ICIs or tyrosine kinase inhibitors (TKIs). These regimens, particularly ICI-based combinations, have significantly improved clinical outcomes and are now established as standard first-line therapies[4]. However, patient responses to immunotherapy remain highly variable, and a substantial proportion of patients exhibit primary resistance or eventually develop acquired resistance. This clinical heterogeneity underscores the urgent, unmet need for robust predictive biomarkers to identify patients most likely to benefit from ICIs and to guide personalized therapeutic strategies[5]. Therefore, the identification of reliable biomarkers to predict immunotherapy response is a critical imperative for optimizing treatment selection and improving outcomes in advanced ccRCC.

We used machine learning method to screen out the key biomarker of ccRCC, paired-like homeodomain 1 (PITX1), which belongs to the bicoid-related homeobox family. The activity of telomerase, a ribonucleoprotein essential for telomere maintenance, cellular immortalization, and cancer progression, is chiefly determined by the expression of telomerase reverse transcriptase (TERT). PITX1 directly binds to the specific PITX1 reaction element site in TERT promoter region, resulting in telomerase inhibition[6, 7]. Previous studies have observed abnormal expression of PITX1 in various tumors, including lung cancer and melanoma[8, 9]. These findings suggest that decreased PITX1 expression induces the activation of oncogenic pathways, thereby promoting cancer development. Unfortunately, the role of PITX1 in the pathogenesis of ccRCC remains largely unknown. Therefore, there is an urgent need to further investigate the function of PITX1 in ccRCC, with particular focus on its potential as a predictor of immunotherapy response.

This study aims to investigate the predictive value of PITX1 in immunotherapy efficacy of advanced ccRCC using multi-omics data. We integrated bulk RNA sequencing (bulk RNA-seq), single-cell RNA sequencing (scRNA-seq), and spatial transcriptomics (ST) to validate the marked upregulation of PITX1 in ccRCC. We further investigated its correlation with metabolic reprogramming, especially glucose metabolism disorders. We focused on the effects of PITX1 on immune and stromal components respectively to reshape the tumor microenvironment (TME). Additionally, data from West China Hospital (WCH), and three randomized controlled trials (RCTs), IMmotion151[10], CheckMate025[11] and JAVELIN Renal 101[12] were analyzed to assess the correlation between PITX1 expression and clinicopathological features and immunotherapy efficacy. Our results indicate that upregulated PITX1 expression serves as an independent prognostic factor for poor survival and predicts inferior responses to ICIs in advanced ccRCC, supporting its potential role as a novel biomarker for risk stratification and therapeutic guidance.

Materials and methods

Machine Learning

"Limma" package was used to conduct a differential expression analysis based on the RNA-seq of IMmotion151 cohort. RNA-seq and prognostic information of IMmotion151 were used to perform

random survival forest (RSF) with number of trees = 1000, splitting rule = log-rank, node size = 5, which is a non-parametric ensemble method for analyzing survival data, it aggregates decision tree predictions to estimate individual survival probabilities and identify significant prognostic factors. RSF was performed by the "randomForestSRC" R package.

Bulk RNA-seq

RNA-seq data of ccRCC tumors and adjacent normal tissues, as well as patient clinical information, were obtained from The Cancer Genome Atlas (TCGA) database. In addition, RNA-seq data of ccRCC tumors and normal kidney tissues were obtained from Gene Expression Omnibus (GEO). RNA-seq was also performed on untreated primary tumors and normal tissues from ccRCC patients who collected and underwent surgery at West China Hospital. This study was approved by the Ethics Committee of data-collecting institution. The method for extracting RNA and generating the expression matrix has been described previously[13]. ComBat algorithm was used to normalize and combine the transcriptome matrices of different sequencing batches in WCH. Transcriptomics data and clinical information were derived from three RCTs. IMmotion151 (NCT02420821)[10], was a phase III trial comparing the efficacy of first-line atezolizumab plus bevacizumab versus sunitinib in untreated patients with metastatic RCC. We only included ccRCC in analysis. CheckMate025 (NCT01668784)[11], was a phase III trial comparing the efficacy of nivolumab versus everolimus in patients with previously treated advanced ccRCC. JAVELIN Renal 101 (NCT02684006)[12], was a phase III trial comparing the efficacy of first-line avelumab plus axitinib versus sunitinib in untreated patients with advanced ccRCC. Patients were stratified according to PITX1 expression, and Kaplan-Meier (KM) survival analysis was used to compare overall survival (OS) and progression-free survival (PFS).

scRNA-seq

Using “Seurat” (v4.3.0), the KIRC_GSE159115 data was performed quality control (cell number > 1000, UMI count per cell > 1000, gene number per cell > 500), batch effect removal, cell clustering, and cell-type annotation. The “Nebulosa” package restores lost gene signals by incorporating similarities between cells, allowing for the convolution of cell characteristics, thereby enabling better visualisation in UMAP. To explore the different expression patterns of PITX1 in various cell clusters, we extracted all cell clusters, identified the expression status of PITX1, divided these cell clusters into two groups based on the positive or negative expression and calculated the proportion of these two groups in each cell cluster.

ST

We integrated previous 10xVisium sequencing to construct a ccRCC ST atlas, including 25 ST slices (KIRC-KIRC25), and the corresponding relationships are shown in “Abbreviations”. The “fromto” package was used to conduct analysis on the standardized data to visually display the gene expression patterns.

We used the “Cottrazm” package to integrate images from KIRC8 (GSE175540-GSM5924036), define tumor boundary, perform spatial deconvolution, and use characteristic genes of cell types in single-cell data to decompose mixed signals in ST data into contributions from different cell types. The grid diagram showing the correlation between PITX1 and different cell types was generated by “linkET” and “ggplot2”[14, 15].

Metabolomics analysis

“METAbolic Flux balance analysis (METAFlux)” package was used to predict metabolite scores from RNA-seq expression profiles of WCH cohort[16]. We divided ccRCC samples in our cohort into PITX1-high and PITX1-low subgroups based on the median expression of PITX1. We used orthogonal partial least squares discriminant analysis (OPLS-DA) statistical method to identify key metabolites that differed between PITX1-high and PITX1-low, and calculated the variable importance in projection (VIP) values[17]. We set VIP > 1 & pvalue < 0.05 as the screening criteria. S-plot was calculated by “MetaboAnalystR” package. And bar chart, Z-score distribution chart and S-plot chart were all visualized by “ggplot2” package. Then we used “clusterProfiler” package to perform metabolite set enrichment analysis (MSEA) by using RaMP-DB (integrating Kyoto encyclopedia of genes and genomes (KEGG), Human Metabolome Database (HMDB), Reactome, WikiPathways) metabolic pathways[18].

Enrichment analysis

Analysis of differentially expressed genes (DEGs) between subgroups was performed using “Limma” package in WCH cohort. R packages “clusterProfiler” was used to perform gene ontology (GO) and KEGG analyses. Gene set enrichment analysis (GSEA) used hallmark and all canonical pathways from molecular signatures database (MSigDB). In addition, “GSVA” package was used to perform single sample GSEA (ssGSEA).

Immune-related analysis

We used immune cell abundance identifier (ImmuCellAI), and “xCell” package to calculate the immune infiltration score for our institution expression profile[19]. Next, tracking tumor immunophenotype (TIP) was used to track and analyse the anti-cancer immune status and tumor-infiltrating immune cells throughout the entire cancer immune cycle[20]. Different T cell states were evaluated by “TCellSI” package[21].

Drug sensitivity analysis

Using the “oncoPredict” package, drug sensitivity analysis was made in our cohort expression profiles based on the genomics of drug sensitivity in cancer (GDSC) and cancer therapeutics response portal

(CTRP) databases, and assessed drug sensitivity by using the half maximal inhibitory concentration (IC50)[22].

Project explanation

Our work has been reported in line with the REMARK criteria[23].

Results

Machine learning identified PITX1 as a key biomarker for ccRCC

BAP1 is an important tumor suppressor gene, which are involved in regulating multiple cellular processes, including DNA damage repair and cell cycle. In ccRCC, the inactivation mutation of BAP1 is one of the most characteristic molecular alterations. BAP1 mutations often lead to higher tumor grades and poorer prognosis[24, 25]. We conducted a differential expression analysis between BAP1-mutant and BAP1-wild based on the RNA-seq of IMmotion151 cohort (Fig. 1A). Then, RSF was performed using the expression matrix of 41 DEGs (p.adj < 0.05, log2 fold change (log2FC) > 1) upregulated in BAP1-mutant group and the PFS data of patients in IMmotion151. RSF results demonstrated the ranking of prognostic predictive importance of different variables (Fig. 1B). The specific parameter settings of RSF model can be found in **Supplementary Table 1**. And the C-index curve of the 10-fold cross-validation of RSF model is shown in **Supplementary Fig. 1A.** We found PITX1 hold the largest proportion of importance, which could be a biomarker significantly associated with the prognosis of ccRCC and related to BAP1 mutation.

In addition, we also conducted a LASSO + COX screening process using 41 DEGs based on IMmotion151, further demonstrating the uniqueness and stability of PITX1 as a biomarker. 9 key signatures were selected via lambda.min using cross-validation, with deviance as the screening criterion (**Supplementary Fig. 1B**). The variation trajectory of LASSO variables also proved the significance of PITX1 (**Supplementary Fig. 1C**). Moreover, univariate and multivariate COX regression analyses were conducted on the 9 genes screened by LASSO, which suggested that PITX1 showed the most significant association, with the highest hazard ratio (HR) and lowest p-value in both univariate and multivariate Cox regression (**Supplementary Fig. 1D, E**).

Bulk RNA-seq analysis revealed that PITX1 is aberrantly upregulated in ccRCC

We initially compared the mRNA expression level of PITX1 between tumor tissues and adjacent normal tissues with TCGA-KIRC data, increased PITX1 expression was observed in tumor tissues ($p < 0.001$, Fig. 1C). In addition, expression profiling data were obtained from a GEO dataset (GSE40435), and the result also showed that PITX1 was upregulated in ccRCC ($p < 0.001$, Fig. 1D). Moreover, we performed

RNA sequencing on samples from WCH (including 150 untreated primary ccRCC and 93 adjacent normal renal tissues) and compared the mRNA expression levels of PITX1 between tumor and normal tissues. As expected, the mRNA expression levels of PITX1 were also significantly elevated in our own cohort ($p < 0.01$, Fig. 1E). We further investigated the correlation of DNA methylation of multiple probes with PITX1 expression between ccRCC samples and normal samples. Probes included cg24495017, cg02948884, cg21614303. Both single probe-based analysis and final aggregation results indicated DNA methylation in ccRCC was significantly lower than in normal samples (all $p < 0.01$, Fig. 1F). The abnormal upregulation of PITX1 may be related to mutational effect of BAP1 and low methylation regulation.

Single-cell analysis revealed PITX1 expression patterns in different cell clusters and impact on biological behavior of tumor cells

After confirming the differential expression of PITX1 at the bulk RNA-seq level, we then conducted verification at the single-cell level. The KIRC_GSE159115 dataset was processed using Seurat (v4.3.0) for quality control, batch effect removal, cell clustering, and cell-type annotation (Fig. 2A). The specific markers for cell annotation are shown in **Supplementary Fig. 1F**. UMAP scatter plots and density plots presented the distribution of PITX1 in different cell clusters, PITX1 was found to be distributed more abundantly in malignant cells (Fig. 2B, C). Comparison of the average PITX1 expression levels among different cell clusters also confirmed it ($p < 0.001$, Fig. 2D). In addition, we isolated the malignant cells to explore the expression pattern of PITX1 in ccRCC tumor cells. The results showed that PITX1 was positively expressed in most malignant cells (79.7%, Fig. 2E). In addition, we explored the impact of PITX1 on biological behavior of malignant cells at the cellular level. A total of 33 cell cluster were obtained through dimensionality reduction clustering (C0-C32), among which malignant cells were classified into eight clusters, including C0, C3, C7, C13, C14, C16, C19, C26 (Fig. 2F). According to the expression of PITX1 in malignant cell clusters, these clusters were divided into PITX1-high cluster (C0, C7, C13, C14, C19, C26) and PITX1-low cluster (C3, C14, C16). The DEGs of PITX1-high cluster compared with PITX1-low cluster were obtained through differential expression analysis (Fig. 2G). Furthermore, we conducted GSEA analysis based on hallmark pathways, and the results suggested that cell proliferation-related pathways such as "MYC Targets V1" and "Mtorc1 Signaling" were enriched in PITX1-high cluster. Glycolysis was also observed to enriched in PITX1-high cluster (Fig. 2H). Overall, PITX1 showed a highly expressed pattern in tumor cells, and tumor cells with elevated expression of PITX1 were often associated with more malignant biological behaviors.

ST revealed cell localization and PITX1 expression differences across spots

By integrating 10x Visium sequencing of KIRC-KIRC25 slices and characterizing the cell types in each region, we named the spots according to the proportion of cell types, distinguishing malignant and non-malignant spots, tumor boundary spots, and various cell type spots within the TME[15]. We standardized the PITX1 expression data of various cells in different ST slices, and the heatmap showed that expression of PITX1 was significantly upregulated in tumor cells than in other type cells (Fig. 3A).

Additionally, we used the “SpatialFeaturePlot” function to combine PITX1 expression information from KIRC8 (GSE175540-GSM5924036) data with spatial location and presented the intensity of PITX1 expression in different spots (Fig. 3B). We then respectively presented KIRC8 (GSE175540-GSM5924036) malignant and non-malignant spots, tumor boundary spots and distribution of various cell type spots (Fig. 3C, D, E). By quantitatively comparing PITX1 expression in different spots, we found that the levels of PITX1 expression in malignant and tumor boundary spots were significantly higher than those in non-malignant spots ($p < 0.001$, Wilcoxon rank sum test, Fig. 3H, I), which were consistent with bulk RNA-seq analysis. Based on the identification of different cell type spots in the TME, we conducted Spearman correlation analysis to assess the relationships between cell content across all spots and between cell content and PITX1 expression levels (Fig. 3J). The results showed that PITX1 expression was positively correlated with $CD8^+$T cells, macrophage and tumor cells, and negatively correlated with endothelial cells and fibroblasts, suggesting the close relationship between PITX1 and anti-tumor immunity. Moreover, the “AUCell” method was used to quantify the expression enrichment degree of specific gene sets in each spot, including "REACTOME_S_PHASE" and "REACTOME_MITOTIC_G2_G2_M_PHASES", the result indicated that cell cycle-related pathways were more enriched in spots with higher expression of PITX1 (Fig. 3F, G). The effects of PITX1 on cell proliferation and the TME deserve more in-depth research.

Increased PITX1 expression was associated with adverse clinicopathologic features and poor prognosis in ccRCC

We collected and curated clinical and pathological data from our institution, including age, gender, tumor size, pT stage, pN stage, pM stage, AJCC stage, and ISUP/WHO grade (**Supplementary Table 2**). The association between PITX1 expression and these parameters was analyzed to investigate its clinical significance in ccRCC. The results demonstrated that PITX1 expression was not correlated with gender or age, but it was significantly positively correlated with tumor size, pT stage, pN stage, pM stage, AJCC stage and ISUP/WHO grade (Fig. 4J). To evaluate the impact of PITX1 expression on prognosis of ccRCC, KM survival analysis was performed. Patients were stratified into PITX1-high and PITX1-low groups based on the median expression value of PITX1 within different cohorts. We separately analyzed the prognostic relationship between PITX1 expression and TCGA OS data ($p < 0.001$, Fig. 4A), IMmotion151 PFS data ($p < 0.001$, Fig. 4B), CheckMate025 PFS & OS data ($p < 0.05$, Fig. 4D, E) and JAVELIN Renal 101 PFS data ($p < 0.05$, Fig. 4H), which suggesting increased PITX1 expression was associated with poorer clinical outcomes.

PITX1 affected tumor metabolism and mediated tumor metabolic reprogramming

METAFlux is a computational approach used to model and analyze the metabolic network of cells or organisms. By integrating genomic, transcriptomic, and metabolomic data, METAFlux predicts the flow of metabolites through metabolic pathways under different conditions. Using this approach, we

predicted metabolite abundance based on RNA-seq expression profiles from WCH cohort. We used OPLS-DA statistical methods to identify key metabolite differences between PITX1-high and PITX1-low group and calculated VIP values. A larger VIP indicates that this metabolite contributes more to the grouping. We set VIP > 1 and p value < 0.05 as the screening criteria and listed these key metabolites in order of p value (Fig. 5B). Figure 5C showed the Z-score distribution of the corresponding metabolite scores for each patient. Based on the S-plot results, methionine, which has the highest VIP value, was significantly negatively correlated with PITX1 expression (Fig. 5D). Alterations in methionine metabolism and abnormal epigenetic regulation are widespread in cancer, helping tumor cells have rapid proliferation and gain growth advantages[26]. Additionally, methionine metabolic crosstalk enables tumor cells to regulate the expression of immune checkpoint expression through methylation modification, thereby evading anti-tumor immunity[27]. Collectively, our findings suggested that PITX1 drives oncogenic processes and shapes the TME by reprogramming methionine metabolism, positioning this essential amino acid as a critical effector of PITX1 function. On the basis of S-plot, acetate, glycerol, linoleate and glucose were enriched in PITX1-low group, while lactate, pyruvate and lysine were enriched in PITX1-high group (Fig. 5D). High-rate glycolysis leading to a large accumulation of lactate could promote PD-1 expression in regulatory T cells (Tregs)[28]. Then perform MSEA with metabolites enriched in PITX1-high group using RaMP-DB metabolic pathways. Combining metabolite abundance and enrichment pathways, aerobic glycolysis, cori cycle, galactose metabolism and glucose metabolism were elevated in PITX1-high group (Fig. 5E). According to the Warburg effect, PITX1-high group exhibited enhanced aerobic glycolysis and relatively diminished tricarboxylic acid cycle (TCA) activity, which is the characteristic of tumors obtaining energy rapidly, achieving malignant proliferation and adapting to TME[29]. Overall, the upregulation of PITX1 was linked to tumor metabolic reprogramming and crosstalk between metabolites and TME.

The association between PITX1 expression and tumor biological behavior

The correlation between PITX1 expression and tumor biological hallmarks was explored mainly through differential expression analysis and enrichment analysis. First, DEGs between PITX1-high and -low group were obtained from the expression profile of our cohort (Fig. 6A). We firstly performed GSEA analysis based on hallmark pathways, which suggesting that increased PITX1 may associate with enhanced cell proliferation and cell cycle regulation, while PITX1-low group had a stronger potential for stimulating tumor angiogenesis (Fig. 6B). Combining the GOKEGG analysis (with p-adjust < 0.05 & |log2FC|>0.5 DEGs) and GSEA analysis based on all canonical pathways, we found that the mitosis regulated pathways and the PD-1 signaling pathway were enriched in PITX1-high group, such as “Mitotic Spindle Checkpoint”, while the extracellular matrix (ECM), collagen-related and angiogenesis pathways were enriched in PITX1-low group, such as “ECM-receptor interaction”, “collagen biosynthetic process” and “VEGF pathway” (Fig. 6D, E). Additionally, lipid metabolism was elevated in PITX1-low group, which was consistent with the result of metabolite abundance prediction analysis (Fig. 6C). ssGSEA analysis further confirmed the above findings (Fig. 6F). Moreover, we compared oncogenic stemness features between

PITX1-high and -low groups and found that PITX1-high group exhibited significantly higher stemness, indicating greater tumor progression potential ($p < 0.001$, Fig. 5A)[30]. In addition, based on the GDSC and CTRP databases, IC50 was calculated to predict differences in drug sensitivity between PITX1-high and -low group. The results showed that PITX1-low group had lower IC50 values for axitinib and sorafenib, which were both vascular endothelial growth factor (VEGF)-targeted tyrosine kinase inhibitors (TKI) drugs (Fig. 7E, F). The results indicated that patients with low expression of PITX1 may have a better therapeutic effect on anti-angiogenic drugs. In general, expression level of PITX1 has a significant impact on biological behavior of ccRCC.

PITX1 upregulation correlated with enhanced immune infiltration and immunogenic activity

Having mentioned the correlation between PITX1 and TME in ST analysis and metabolomics analysis, we next utilized transcriptomic data from our cohort to investigate the relationship between PITX1 expression and anti-tumor immunity. First, we calculated immune cell infiltration using two algorithms, ImmuCellAI and xCell, and found that most antigen-presenting cells (APCs), such as macrophages and dendritic cells (DCs), were more abundant in PITX1-high group. Additionally, lymphocytes, including $CD4^+$T cells, $CD8^+$T cells and B cells, were more enriched in this group. The overall TME immune score of PITX1-high group from xCell was also significantly higher. In contrast, stromal cells including endothelial cells have elevated abundance in PITX1-low group. As expected, stroma score of PITX1-low was significantly increased compared to PITX1-high. Notably, natural Tregs (nTregs), induced Tregs (iTregs), and exhausted T cells were all more elevated in PITX1-high group, which indicated that increased expression of PITX1 may exert the immunosuppressive effect through highly infiltrated Treg cells, thereby leading to immune escape (Fig. 7A)[31]. Moreover, by tracking and analyzing the anti-cancer immune status throughout the entire cancer immune cycle using TIP, we found that PITX1 expression levels were significantly positively correlated with tumor antigen presentation, $CD8^+$T cell recruitment and recognition of cancer cell by T cells (Fig. 7B). In addition, predictions from the “TCellSI” package indicated that T cells in PITX1-high group were more likely to exhibit functional states such as proliferation, which were associated with strong anti-tumor activity. However, T cells in senescence and exhaustion states, which were both unfavorable for anti-tumor responses, were also more prevalent in this group (Fig. 7C). Furthermore, PD-1, TIGIT and LAG3 were significantly higher in PITX1-high compared to PITX1-low at mRNA expression level ($p < 0.05$, Fig. 7D). The general elevation of immune checkpoints may be the reason for PITX1-high ccRCC evading immune surveillance and the poor efficacy of immunotherapy. Overall, PITX1-high group was associated with the infiltrated-inflamed tumor immune microenvironment, characterized by high immune cell infiltration, elevated immune activation and upregulation of immune checkpoint. However, the extensive infiltration of Tregs may represent a key factor limiting the effectiveness of tumor immunotherapy.

PITX1 expression may serve as a predictor of immunotherapy response in ccRCC

We utilized data from three RCTs, IMmotion151, CheckMate025 and JAVELIN Renal 101 to assess whether PITX1 can predict and differentiate the efficacy of immunotherapy. We divided patients in cohorts into PITX1-high and PITX1-low group based on PITX1 expression levels. In the CheckMate025 cohort, patients with advanced ccRCC who had previously received anti-angiogenic therapy were included[11]. We selected those who received nivolumab treatment. The results indicated that patients in PITX1-high group receiving nivolumab had significantly inferior PFS ($p < 0.05$) and OS ($p < 0.01$) (Fig. 4F, G). We further investigated whether PITX1 expression could predict the efficacy of combination therapy involving immunotherapy and anti-angiogenic drugs. In the IMmotion151 cohort, we selected untreated patients with metastatic ccRCC who received first-line treatment with atezolizumab plus bevacizumab, which is a combination therapy of immunotherapy and anti-angiogenic drugs[10]. PITX1-high group achieved poorer PFS compared PITX1-low group ($p < 0.001$, Fig. 4C). Moreover, in the JAVELIN Renal 101 cohort, we included untreated patients with advanced ccRCC who received first-line treatment with avelumab plus axitinib, which is also a combination therapy of immunotherapy and anti-angiogenic drugs[12]. As expected, patients in PITX1-high group had significantly worse PFS ($p < 0.001$, Fig. 4I). Taken together, PITX1 expression has been confirmed to be a robust predictive biomarker for immunotherapy in ccRCC.

Discussion

In this study, using the machine learning approach, we identified PITX1 as a top prognostic gene in ccRCC from the IMmotion151 cohort. Validation across multiple bulk RNA-seq datasets, including TCGA-KIRC, GEO, and our institutional cohort, consistently confirmed the upregulation of PITX1 in tumor tissues. Single-cell and spatial transcriptomic analyses further localized PITX1 overexpression predominantly within malignant cells and revealed its association with proliferative and metabolic pathways. Clinically, high PITX1 expression correlated with advanced tumor stage, higher histological grade, and poorer survival across multiple independent cohorts, including three RCTs (IMmotion151, CheckMate025, and JAVELIN Renal 101). Functionally, PITX1 was associated with altered methionine metabolism, enhanced aerobic glycolysis and an immunosuppressive TME characterized by Tregs infiltrated and immune checkpoint upregulated. The multi-omics approach overcame single-method limitations by integrating scRNA-seq and spatial transcriptomics to pinpoint gene expression within specific cells and tumor boundary regions. This convergence of evidence directly tied the gene's expression to underlying biological mechanisms. Our findings provide compelling evidence that PITX1 may serve as a novel predictive biomarker for risk stratification and therapeutic decision-making in advanced ccRCC.

Previous studies have reported that telomerase is crucial for cell immortality and the progression of cancer. Both human TERT and mouse TERT promoter activities can be inhibited by PITX1, which inhibits TERT transcription by directly binding to TERT promoter, ultimately regulating telomerase activity[7]. Our results are consistent with previous studies reporting aberrant PITX1 expression in other malignancies, such as melanoma, where it has been implicated in tumor suppression. However, its role in ccRCC has remained largely unexplored. The association between PITX1 and BAP1 mutation is particularly

noteworthy, as BAP1 loss is a well-established driver of aggressive ccRCC. Our data suggest that PITX1 may act as a downstream effector of BAP1 mutation, contributing to telomerase inhibition and genomic instability, a hypothesis supported by the observed hypomethylation of PITX1 regulatory regions. However, expression of PITX1 is negatively correlated with cell proliferation of cutaneous malignant melanoma, which differs from our findings[9]. We think this may be related to the dual identity of PITX1, namely the oncogene-cooperating factor and the tumor-suppressive role. PITX1 may play more of the role of an oncogene cofactor in ccRCC[32]. In addition, the difference in specific driving mechanisms of cancer and the difference in TME may also be the reasons.

Moreover, the link between PITX1 and metabolic reprogramming aligns with the known Warburg effect in ccRCC. The substantial accumulation of lactate, a consequence of high glycolysis flux, inhibits T cell activity[33]. Our metabolomic analyses revealed that PITX1-high group exhibited enhanced aerobic glycolysis, methionine metabolism and reduced TCA and oxidative phosphorylation, all of which are critical for tumor progression and immune evasion.

From a clinical perspective, PITX1 expression may serve as a valuable biomarker to identify ccRCC patients who are less likely to benefit from immunotherapy. Our analysis of three RCTs consistently showed that high PITX1 expression predicts inferior PFS and OS in patients treated with ICIs, either as monotherapy or in combination with anti-angiogenic agents. Considering the prognostic impact caused by possible differences in treatment methods, we also conducted a risk stratification analysis of PITX1 in TCGA-KIRC and found that PITX1 can indeed predict the prognosis of advanced ccRCC. This suggests that PITX1 could be integrated into existing risk stratification models to optimize treatment selection. For instance, in a hypothetical clinical scenario, patients with high PITX1 expression, who exhibit an immunosuppressive TME and poor response to ICIs, might be directed toward alternative or combined therapeutic strategies, such as TKI or novel immunomodulatory agents. Conversely, patients with low PITX1 expression, who show better response to ICIs, could be prioritized for immunotherapy-based regimens. Such a PITX1-informed stratification could help tailor first-line therapy, reduce unnecessary exposure to ineffective treatments, and ultimately improve clinical outcomes.

Biologically, PITX1 appears to promote an immunosuppressive TME by enhancing Treg infiltration and upregulating immune checkpoints such as PD-1, TIGIT, and LAG3. Despite increased immune cell infiltration, the functional exhaustion of T cells in PITX1-high tumors likely explains the limited efficacy of immunotherapy. Additionally, the association between PITX1 and VEGF pathway activity suggests that PITX1-low tumors may be more responsive to anti-angiogenic therapies, providing a rationale for therapy selection based on PITX1 status.

Several limitations of our study should be acknowledged. First, although we utilized multiple independent cohorts, the retrospective nature of the analysis introduces potential biases. Second, the functional mechanisms through which PITX1 regulates metabolism and immune evasion remain largely inferred from transcriptomic and metabolomic data. Future studies using in vitro and in vivo models are needed to validate these mechanisms experimentally. Future research should focus on elucidating the

transcriptional regulation of PITX1, its interaction with BAP1, and its role in metabolic-immune crosstalk. Additionally, exploring therapeutic strategies to target PITX1 or its downstream pathways may offer new avenues for treating high-risk ccRCC.

Conclusion

In conclusion, we identified PITX1 as a novel biomarker upregulated in ccRCC that is associated with aggressive tumor behavior, metabolic reprogramming, and an immunosuppressive microenvironment. Its ability to predict poor response to immunotherapy across multiple clinical trials underscores its potential clinical value. PITX1, as a therapeutic biomarker, may enable more personalized treatment strategies for patients with advanced ccRCC.

Abbreviations

APCs
Antigen-Presenting Cells
BAP1
BRCA1 Associated Deubiquitinase 1
ccRCC
Clear Cell Renal Cell Carcinoma
CTRP
Cancer Therapeutics Response Portal
DEGs
Differentially Expressed Genes
ECM
Extracellular Matrix
GDSC
Genomics of Drug Sensitivity in Cancer
GEO
Gene Expression Omnibus
GO
Gene Ontology
GSEA
Gene Set Enrichment Analysis
HMDB
Human Metabolome Database
HR
hazard ratio,IC50,Half Maximal Inhibitory Concentration
ICIs
Immune Checkpoint Inhibitors
ImmuCellAI

Immune Cell Abundance Identifier
ITH
Intra-Tumor Heterogeneity
KEGG
Kyoto Encyclopedia of Genes and Genomes
KM
Kaplan-Meier
MSEA
Metabolite Set Enrichment Analysis
MSigDB
Molecular Signatures Database
OPLS-DA
Orthogonal Partial Least Squares Discriminant Analysis
OS
Overall Survival
PD-1
Programmed Cell Death Protein 1
PFS
Progression-Free Survival
PITX1
Paired-Like Homeodomain 1
RCTs
Randomized Controlled Trials
RSF
Random Survival Forest
scRNA-seq
single-cell RNA-seq
ssGSEA
single sample GSEA
ST
Spatial Transcriptomics
TCA
Tricarboxylic Acid Cycle
TCGA
The Cancer Genome Atlas
TERT
Telomerase Reverse Transcriptase
TIP
Tracking Tumor Immunophenotype
TKI

Tyrosine Kinase Inhibitors
TME
Tumor Microenvironment
Tregs
regulatory T cells
VEGF
Vascular Endothelial Growth Factor
VIP
Variable Importance in Projection

Declarations

Ethics Approval and Consent to Participate

This study was conducted in compliance with the Declaration of Helsinki and received approval from the Ethics Committee of West China Hospital, Sichuan University (number: 2022-271). All patients or family members provided written consent for RNA-seq before enrollment.

Consent for Publication

Each author approved the manuscript before submission for publication.

Data Availability

TCGA-KIRC:https://www.cancer.gov/ccg/research/genome-sequencing/tcga/studied-cancers/clear-cell-renal-carcinoma-study;

scRNA-seq: https://ncbi.nlm.nih.gov/geo/query/acc.cgi (GEO accession: GSE159115);

spatial transcriptomics: https://ncbi.nlm.nih.gov/geo/query/acc.cgi (GEO accession: GSE175540);

IMmotion151:https://www.sciencedirect.com/science/article/pii/S0140673619307238?via%3Dihubl;

CheckMate025: https://pmc.ncbi.nlm.nih.gov/articles/PMC5719487/;

JAVELIN Renal 101: https://www.nejm.org/doi/full/10.1056/NEJMoa1816047;

RaMP-DB: https://rampdb.nih.gov/biochemical-pathways;

GOKEGG:https://www.gsea-msigdb.org/gsea/msigdb/human/genesets.jsp?collection=C5;

Reactome:https://www.gsea-msigdb.org/gsea/msigdb/human/genesets.jsp?collection=CP:REACTOME;

WikiPathways:https://www.gsea-msigdb.org/gsea/msigdb/human/genesets.jsp?collection=CP:WIKIPATHWAYS;

MSigDB: https://www.gsea-msigdb.org/gsea/msigdb;

GDSC: https://www.cancerrxgene.org/;

HMDB: https://hmdb.ca/metabolites;

CTRP: https://portals.broadinstitute.org/ctrp/;

The sequencing data are available by contacting the corresponding author upon

reasonable request.

Competing Interests

Not applicable.

Funding

This work was supported by the 1.3.5 project for disciplines of excellence, West China Hospital, Sichuan University (ZYAI24062), "Qimingxing" Research Fund for Young Talents of West China Hospital(HXQMX0046)

Authors' Contributions

Dingbang Liu: Formal analysis, Resources, Methodology, Visualization, Writing-Original Draft, Junjie Zhao: Statistical analyses, Zilin Wang: Software, Yanfeng Tang: Data Curation, Hao Zeng: Supervision, Writing - Review & Editing, Funding acquisition, Jiayu Liang: Supervision, Investigation, Writing-Review & Editing, Funding acquisition. All authors read and approved the final manuscript.

Acknowledgements

The authors thank all patients who participated in this study, as well as their families/caregivers.

References

1. Siegel RL, Giaquinto AN, Jemal A, Cancer statistics. 2024. CA Cancer J Clin. 2024;74(1):12–49. 10.3322/caac.21820
2. Bukavina L, Bensalah K, Bray F, et al. Epidemiology of Renal Cell Carcinoma: 2022 Update. Eur Urol. 2022;82(5):529–42. 10.1016/j.eururo.2022.08.019.
3. Powles T, Albiges L, Bex A, et al. Renal cell carcinoma: ESMO Clinical Practice Guideline for diagnosis, treatment and follow-up. Ann Oncol. 2024;35(8):692–706. 10.1016/j.annonc.2024.05.537.
4. Choueiri TK, Motzer RJ. Systemic Therapy for Metastatic Renal-Cell Carcinoma. N Engl J Med. 2017;376(4):354–66. 10.1056/NEJMra1601333.

5. Li Y, Lih TM, Dhanasekaran SM, et al. Histopathologic and proteogenomic heterogeneity reveals features of clear cell renal cell carcinoma aggressiveness. Cancer Cell. 2023;41(1):139–e16317. 10.1016/j.ccell.2022.12.001.
6. Ohira T, Nakagawa S, Takeshita J, Aburatani H, Kugoh H. PITX1 inhibits the growth and proliferation of melanoma cells through regulation of SOX family genes. Sci Rep. 2021;11(1):18405. Published 2021 Sep 15. 10.1038/s41598-021-97791-6
7. Qi DL, Ohhira T, Fujisaki C, et al. Identification of PITX1 as a TERT suppressor gene located on human chromosome 5. Mol Cell Biol. 2011;31(8):1624–36. 10.1128/MCB.00470-10.
8. Chen Y, Knösel T, Ye F, Pacyna-Gengelbach M, Deutschmann N, Petersen I. Decreased PITX1 homeobox gene expression in human lung cancer. Lung Cancer. 2007;55(3):287–94. 10.1016/j.lungcan.2006.11.001.
9. Osaki M, Chinen H, Yoshida Y, et al. Decreased PITX1 gene expression in human cutaneous malignant melanoma and its clinicopathological significance. Eur J Dermatol. 2013;23(3):344–9. 10.1684/ejd.2013.2021.
10. Rini BI, Powles T, Atkins MB, et al. Atezolizumab plus bevacizumab versus sunitinib in patients with previously untreated metastatic renal cell carcinoma (IMmotion151): a multicentre, open-label, phase 3, randomised controlled trial. Lancet. 2019;393(10189):2404–15. 10.1016/S0140-6736(19)30723-8.
11. Motzer RJ, Escudier B, McDermott DF, et al. Nivolumab versus Everolimus in Advanced Renal-Cell Carcinoma. N Engl J Med. 2015;373(19):1803–13. 10.1056/NEJMoa1510665.
12. Motzer RJ, Penkov K, Haanen J, et al. Avelumab plus Axitinib versus Sunitinib for Advanced Renal-Cell Carcinoma. N Engl J Med. 2019;380(12):1103–15. 10.1056/NEJMoa1816047.
13. Zhao J, Pan X, Wang Z et al. Epigenetic modification of PHLDA2 is associated with tumor microenvironment and unfavorable outcome of immune checkpoint inhibitor-based therapies in clear cell renal cell carcinoma. Eur J Med Res. 2024;29(1):378. Published 2024 Jul 20. 10.1186/s40001-024-01939-9
14. Shi J, Wei X, Xun Z, et al. The Web-Based Portal SpatialTME Integrates Histological Images with Single-Cell and Spatial Transcriptomics to Explore the Tumor Microenvironment. Cancer Res. 2024;84(8):1210–20. 10.1158/0008-5472.CAN-23-2650.
15. Xun Z, Ding X, Zhang Y, et al. Reconstruction of the tumor spatial microenvironment along the malignant-boundary-nonmalignant axis. Nat Commun. 2023;14(1):933. 10.1038/s41467-023-36560-7. Published 2023 Feb 20.
16. Huang Y, Mohanty V, Dede M, et al. Characterizing cancer metabolism from bulk and single-cell RNA-seq data using METAFlux. Nat Commun. 2023;14(1):4883. 10.1038/s41467-023-40457-w. Published 2023 Aug 12.
17. Kang C, Zhang Y, Zhang M, et al. Screening of specific quantitative peptides of beef by LC-MS/MS coupled with OPLS-DA. Food Chem. 2022;387:132932. 10.1016/j.foodchem.2022.132932.

18. Braisted J, Patt A, Tindall C, et al. RaMP-DB 2.0: a renovated knowledgebase for deriving biological and chemical insight from metabolites, proteins, and genes. Bioinformatics. 2023;39(1):btac726. 10.1093/bioinformatics/btac726.
19. Miao YR, Zhang Q, Lei Q, et al. ImmuCellAI: A Unique Method for Comprehensive T-Cell Subsets Abundance Prediction and its Application in Cancer Immunotherapy. Adv Sci (Weinh). 2020;7(7):1902880. 10.1002/advs.201902880. Published 2020 Feb 11.
20. Xu L, Deng C, Pang B, et al. TIP: A Web Server for Resolving Tumor Immunophenotype Profiling. Cancer Res. 2018;78(23):6575–80. 10.1158/0008-5472.CAN-18-0689.
21. Yang JM, Zhang N, Luo T, et al. TCellSI: A novel method for T cell state assessment and its applications in immune environment prediction. Imeta. 2024;3(5):e231. 10.1002/imt2.231. Published 2024 Aug 26.
22. Maeser D, Gruener RF, Huang RS. oncoPredict: an R package for predicting in vivo or cancer patient drug response and biomarkers from cell line screening data. Brief Bioinform. 2021;22(6):bbab260. 10.1093/bib/bbab260.
23. McShane LM, Altman DG, Sauerbrei W, et al. REporting recommendations for tumour MARKer prognostic studies (REMARK). Br J Cancer. 2005;93(4):387–91. 10.1038/sj.bjc.6602678.
24. Carbone M, Harbour JW, Brugarolas J, et al. Biological Mechanisms and Clinical Significance of BAP1 Mutations in Human Cancer. Cancer Discov. 2020;10(8):1103–20. 10.1158/2159-8290.CD-19-1220.
25. Walton J, Lawson K, Prinos P, Finelli A, Arrowsmith C, Ailles L. PBRM1, SETD2 and BAP1 - the trinity of 3p in clear cell renal cell carcinoma. Nat Rev Urol. 2023;20(2):96–115. 10.1038/s41585-022-00659-1.
26. Bin P, Wang C, Zhang H, Yan Y, Ren W. Targeting methionine metabolism in cancer: opportunities and challenges. Trends Pharmacol Sci. 2024;45(5):395–405. 10.1016/j.tips.2024.03.002.
27. Sanderson SM, Gao X, Dai Z, Locasale JW. Methionine metabolism in health and cancer: a nexus of diet and precision medicine. Nat Rev Cancer. 2019;19(11):625–37. 10.1038/s41568-019-0187-8.
28. Kumagai S, Koyama S, Itahashi K, et al. Lactic acid promotes PD-1 expression in regulatory T cells in highly glycolytic tumor microenvironments. Cancer Cell. 2022;40(2):201–e2189. 10.1016/j.ccell.2022.01.001.
29. Icard P, Shulman S, Farhat D, Steyaert JM, Alifano M, Lincet H. How the Warburg effect supports aggressiveness and drug resistance of cancer cells? Drug Resist Updat. 2018;38:1–11. 10.1016/j.drup.2018.03.001.
30. Chen D, Liu J, Zang L, et al. Integrated Machine Learning and Bioinformatic Analyses Constructed a Novel Stemness-Related Classifier to Predict Prognosis and Immunotherapy Responses for Hepatocellular Carcinoma Patients. Int J Biol Sci. 2022;18(1):360–73. 10.7150/ijbs.66913. Published 2022 Jan 1.
31. Kumagai S, Itahashi K, Nishikawa H. Regulatory T cell-mediated immunosuppression orchestrated by cancer: towards an immuno-genomic paradigm for precision medicine. Nat Rev Clin Oncol.

2024;21(5):337–53. 10.1038/s41571-024-00870-6.

32. Falcomatà C, Bärthel S, Schneider G, Rad R, Schmidt-Supprian M, Saur D. Context-Specific Determinants of the Immunosuppressive Tumor Microenvironment in Pancreatic Cancer. Cancer Discov. 2023;13(2):278–97. 10.1158/2159-8290.CD-22-0876.
33. Elia I, Rowe JH, Johnson S, et al. Tumor cells dictate anti-tumor immune responses by altering pyruvate utilization and succinate signaling in CD8 + T cells. Cell Metab. 2022;34(8):1137–e11506. 10.1016/j.cmet.2022.06.008.

Figures

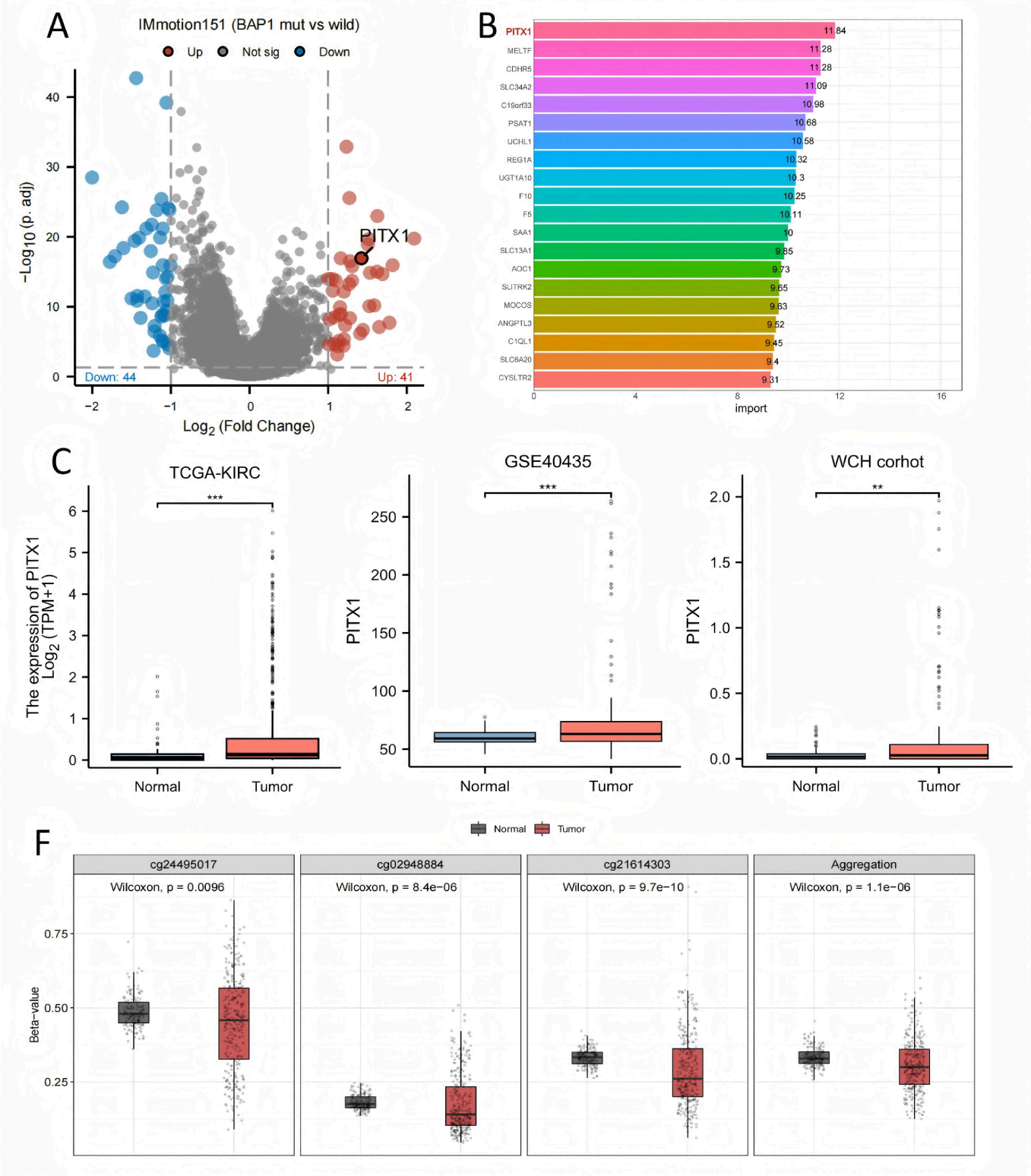


Figure 1

Machine learning screening and expression pattern of PITX1 in ccRCC. (A) Differential expression analysis between BAP1-mutant and BAP1-wild based on the RNA-seq of IMmotion151 cohort. **(B)** Using the expression matrix of DEGs (p.adj<0.05, log2FC>1) upregulated in BAP1-mutant group and PFS data in IMmotion151 to perform RSF. **(C)** mRNA expression level of PITX1 between paired tumor and normal tissues based on TCGA-KIRC database. **(D)** mRNA expression level of PITX1 between tumor and normal

tissues based on GSE40435. **(E)** mRNA expression level of PITX1 between tumor (n=150) and normal tissues (n=93) in ccRCC based on WCH cohort. **(F)** DNA methylation of multiple probes with PITX1 expression between ccRCC and normal samples. DEGs, Differentially Expressed Genes. *p<0.05, **p<0.01, ***p<0.001.

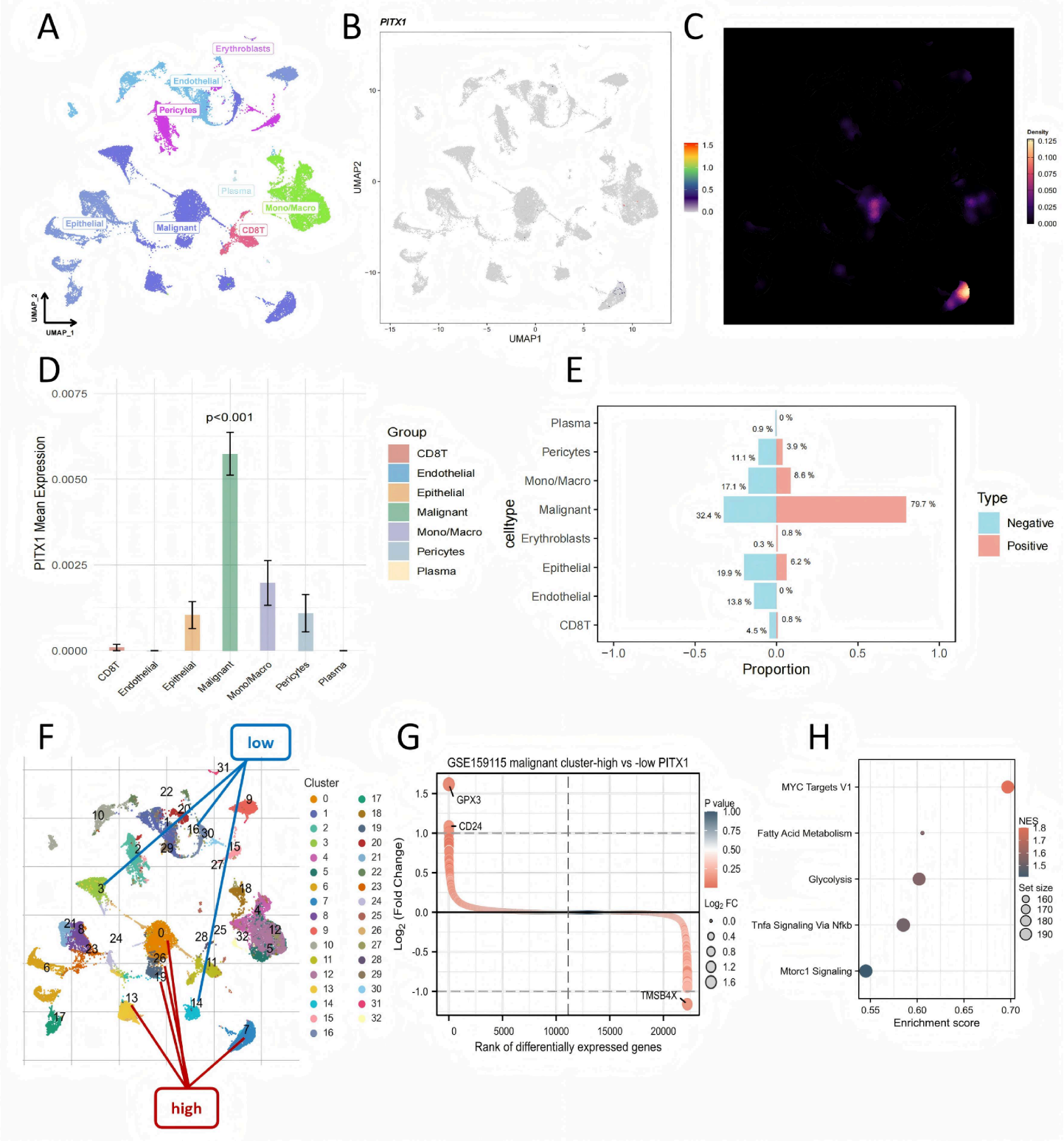


Figure 2

Single-cell analysis of PITX1. (A) UMAP plots of cell clustering annotation based on KIRC_GSE159115 dataset. **(B)** UMAP plots of PITX1 expression distribution. **(C)** Density plots of PITX1 expression distribution. **(D)** Mean PITX1 expression levels among different cell clusters. **(E)** Proportion of positive and negative PITX1 in different cell clusters. **(F)** Total of 33 cell cluster (C0-C32), malignant cells included C0, C3, C7, C13, C14, C16, C19, C26, which were divided into PITX1-high cluster (C0, C7, C13, C19, C26) and PITX1-low cluster (C3, C14, C16). **(G)** The DEGs of PITX1-high cluster compared with PITX1-low cluster. **(H)** GSEA analysis based on hallmark pathways based on the DEGs. GSEA, Gene Set Enrichment Analysis.

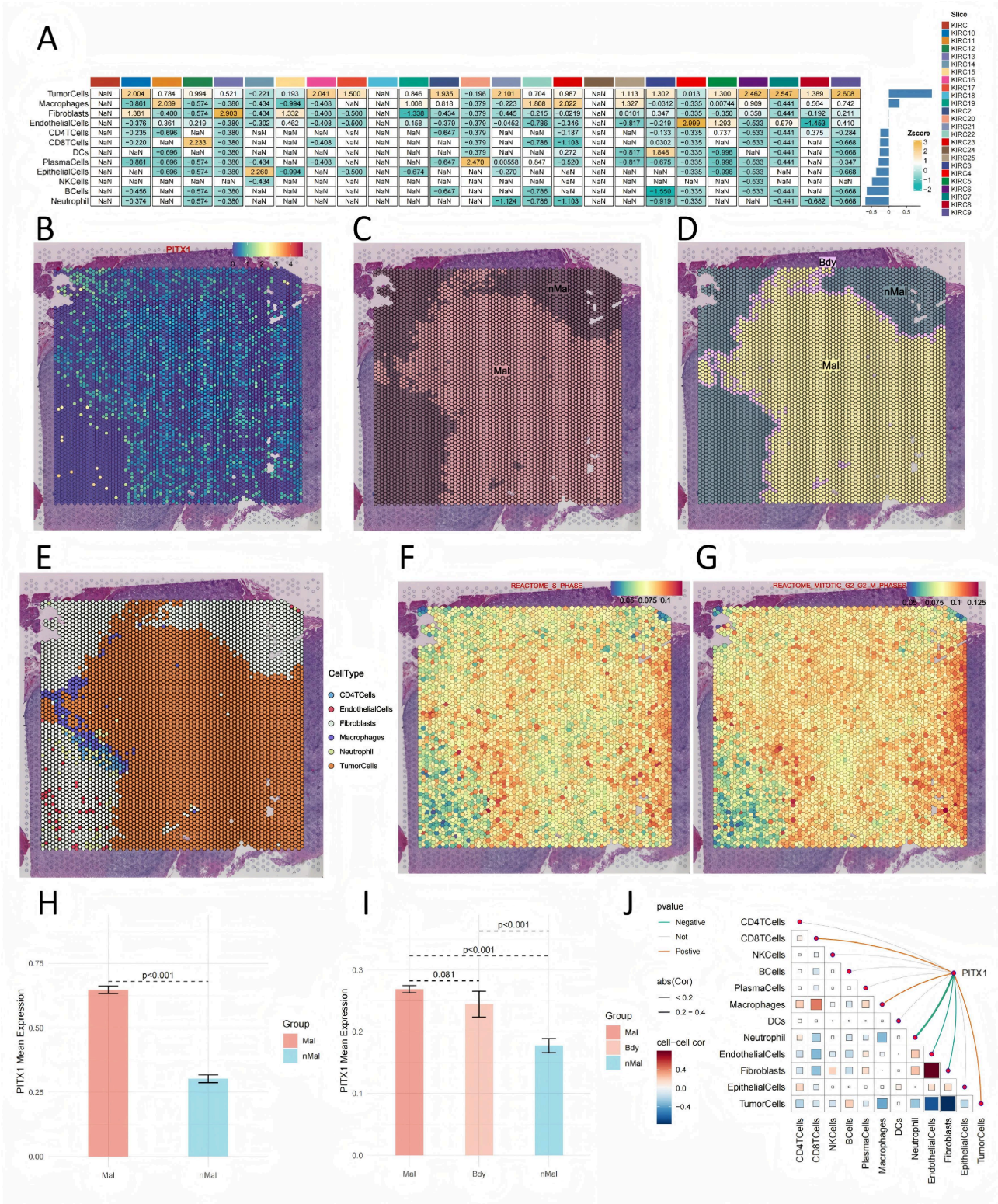


Figure 3

Spatial transcriptomics analysis of PITX1. (A) Heatmap showed PITX1 expression of various cells in KIRC-KIRC25 ST slices. **(B)**Intensity of PITX1 expression in different spots based on KIRC8 (GSE175540-GSM5924036). **(C)** KIRC8 (GSE175540-GSM5924036) identified as malignant and non-malignant spots. **(D)** KIRC8 identified as malignant, non-malignant and tumor boundary spots. **(E)** KIRC8 identified as various cell type spots. **(F)** Quantify the expression enrichment degree of "REACTOME_S_PHASE" in each

spot by using “AUCell” method. **(G)** Quantify the expression enrichment degree of "REACTOME_MITOTIC_G2_G2_M_PHASES" in each spot by using “AUCell” method. **(H)** Compared PITX1 expression in malignant and non-malignant spots. **(I)** Compared PITX1 expression in malignant, non-malignant and tumor boundary spots. **(J)** Correlation among different cell content across all spots and between cell content and PITX1 expression levels.

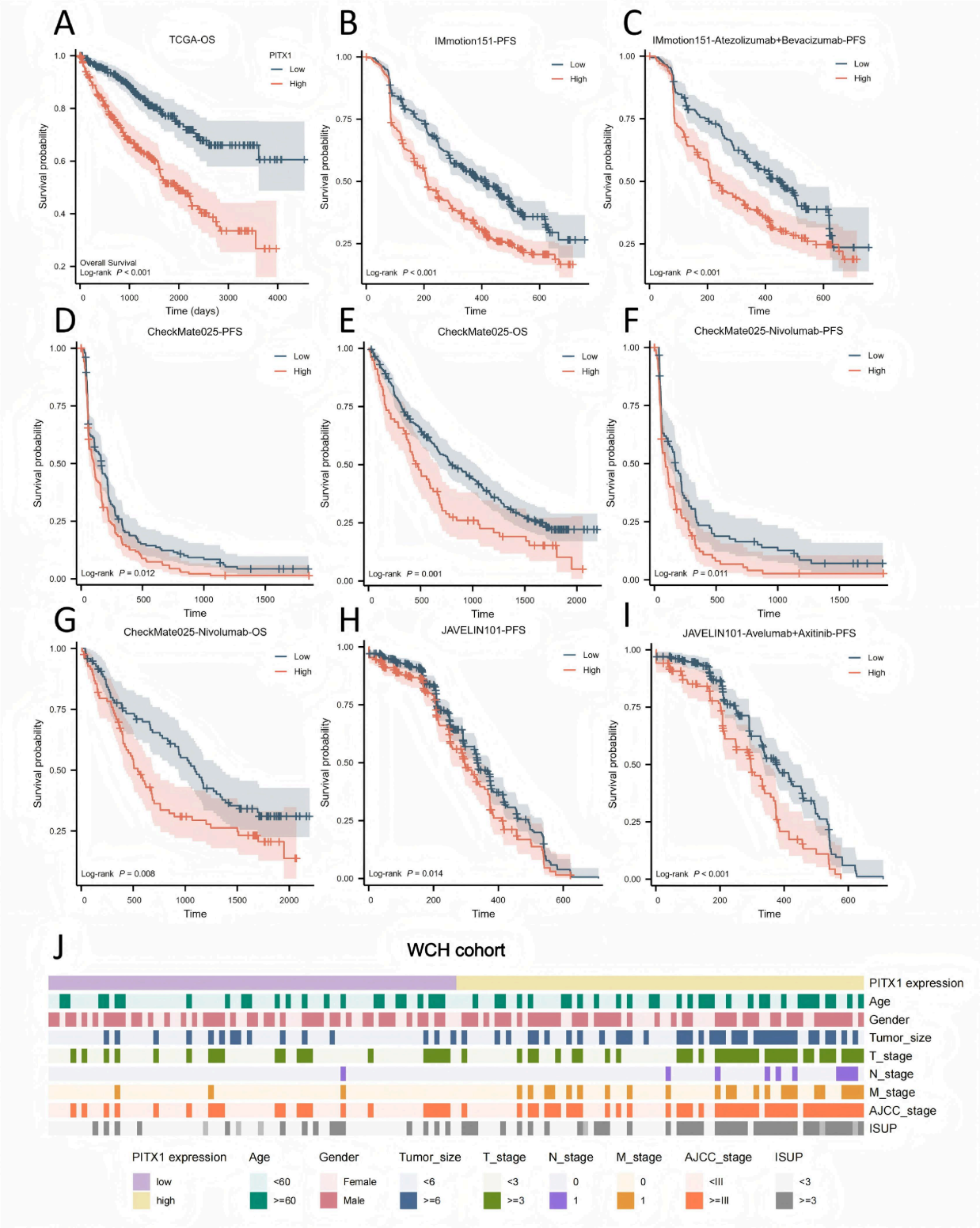


Figure 4

Correlations with clinicopathologic parameters and prognosis of PITX1 in ccRCC. (A) OS of ccRCC patients in PITX1-high and PITX1-low subgroups in TCGA cohort by Kaplan-Meier survival analysis. **(B)** PFS of ccRCC patients in PITX1-high and PITX1-low subgroups in IMmotion151 cohort by Kaplan-Meier survival analysis. **(C)** PFS of ccRCC patients treated with atezolizumab plus bevacizumab in PITX1-high and PITX1-low subgroups in IMmotion151 cohort by Kaplan-Meier survival analysis. **(D)** PFS of ccRCC patients in PITX1-high and PITX1-low subgroups in CheckMate025 cohort by Kaplan-Meier survival analysis. **(E)** OS of ccRCC patients in PITX1-high and PITX1-low subgroups in CheckMate025 cohort by Kaplan-Meier survival analysis. **(F)** PFS of ccRCC patients treated with nivolumab in PITX1-high and PITX1-low subgroups in CheckMate025 cohort by Kaplan-Meier survival analysis. **(G)** OS of ccRCC patients treated with nivolumab in PITX1-high and PITX1-low subgroups in CheckMate025 cohort by Kaplan-Meier survival analysis. **(H)** PFS of ccRCC patients in PITX1-high and PITX1-low subgroups in JAVELIN Renal 101 cohort by Kaplan-Meier survival analysis. **(I)** PFS of ccRCC patients treated with avelumab plus axitinib in PITX1-high and PITX1-low subgroups in JAVELIN Renal 101 cohort by Kaplan-Meier survival analysis. **(J)** Distribution of clinicopathological features from WCH cohort in PITX1-high and PITX1-low subgroups. OS, Overall Survival; PFS, Progression-Free Survival.

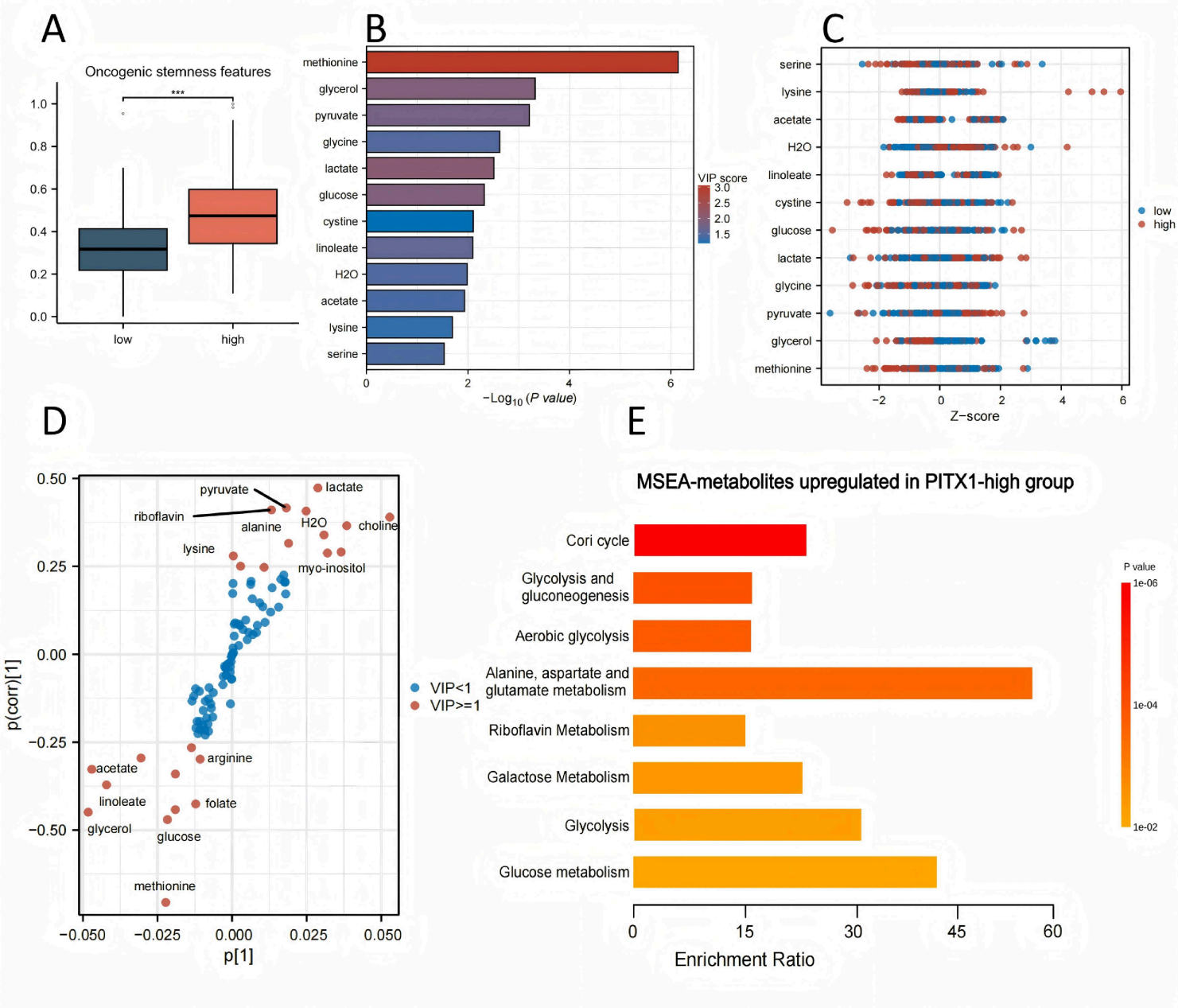


Figure 5

Metabolomics analysis of PITX1. (A) Comparison of oncogenic stemness features between PITX1-high and PITX1-low groups. Based on the human stem cell dataset provided by the Progenitor Cell Biology Consortium (PCBC), the stemness of tumor cells was quantified using One-class Linear Regression (OCLR). **(B)** Bar chart listed key metabolites with VIP > 1 and p value < 0.05. **(C)** Z-score distribution of these key metabolites. **(D)** S-plot showed the correlation between different metabolites and expression of PITX1. The x-axis is the covariance, which represented the strength of the relationship between metabolites and PITX1 expression; the y-axis is the correlation, which represented the strength of the linear relationship between metabolites and PIXT1 expression. **(E)** MSEA with metabolites enriched in PITX1-high group using RaMP-DB metabolic pathways. The above analysis is based on “METAFlux” to predict the abundance of metabolites and OPLS-DA method was used to compare metabolite

differences. VIP, Variable Importance in Projection; MSEA, Metabolite Set Enrichment Analysis; OPLS-DA, Orthogonal Partial Least Squares Discriminant Analysis. *p<0.05, **p<0.01, ***p<0.001.

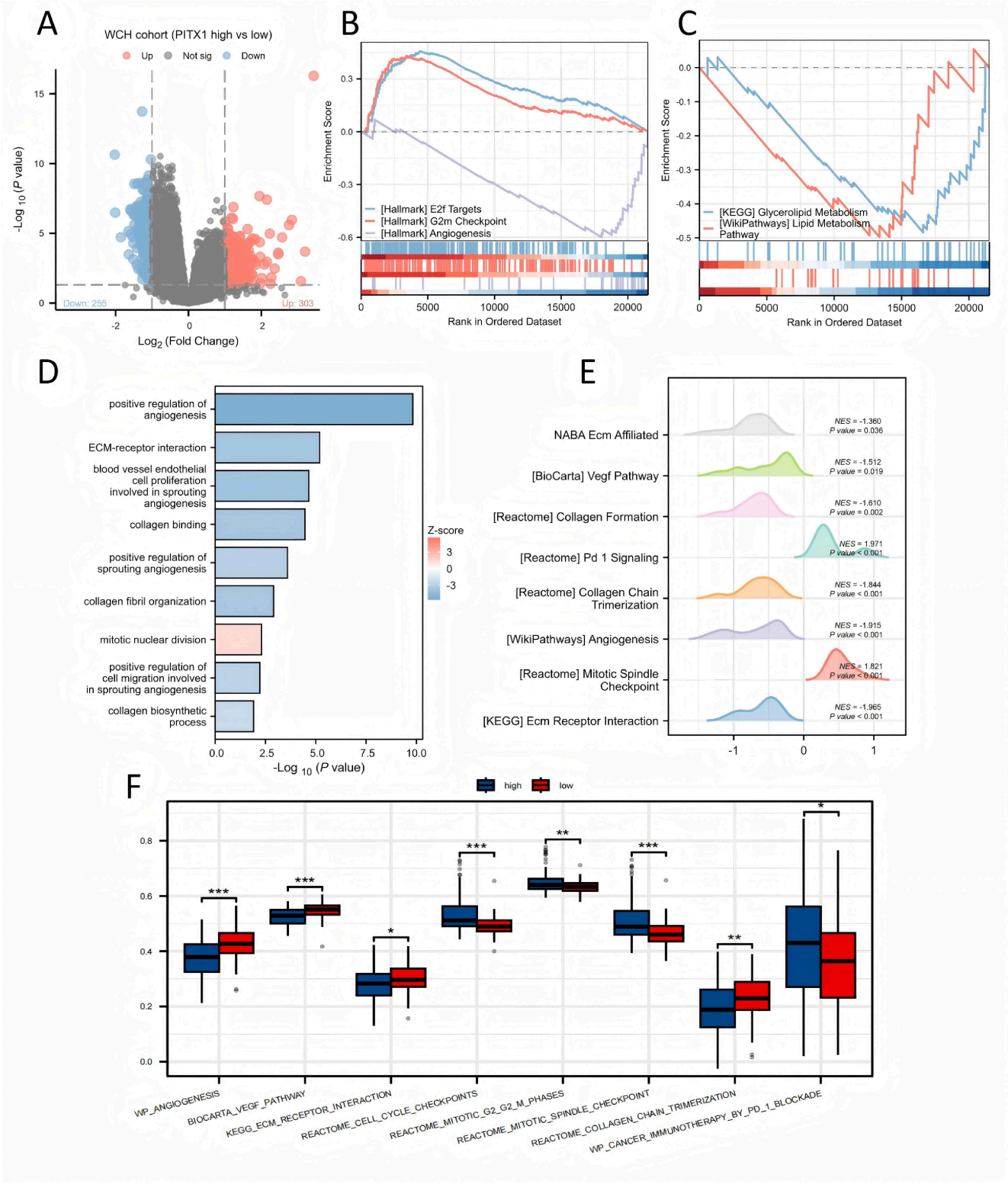


Figure 6

Enrichment analysis related to PITX1 expression. (A) DEGs between PITX1-high and -low group from the expression profile of WCH cohort. **(B, C)** GSEA analysis based on hallmark pathways. **(D)** GOKEGG

analysis (with p-adjust<0.05 & |log2FC|>0.5 DEGs). **(E)** GSEA analysis based on all canonical pathways. **(F)** ssGSEA analysis between PITX1-high and PITX1-low groups. All pathways are from Molecular Signatures Database (MSigDB). *p<0.05, **p<0.01, ***p<0.001.

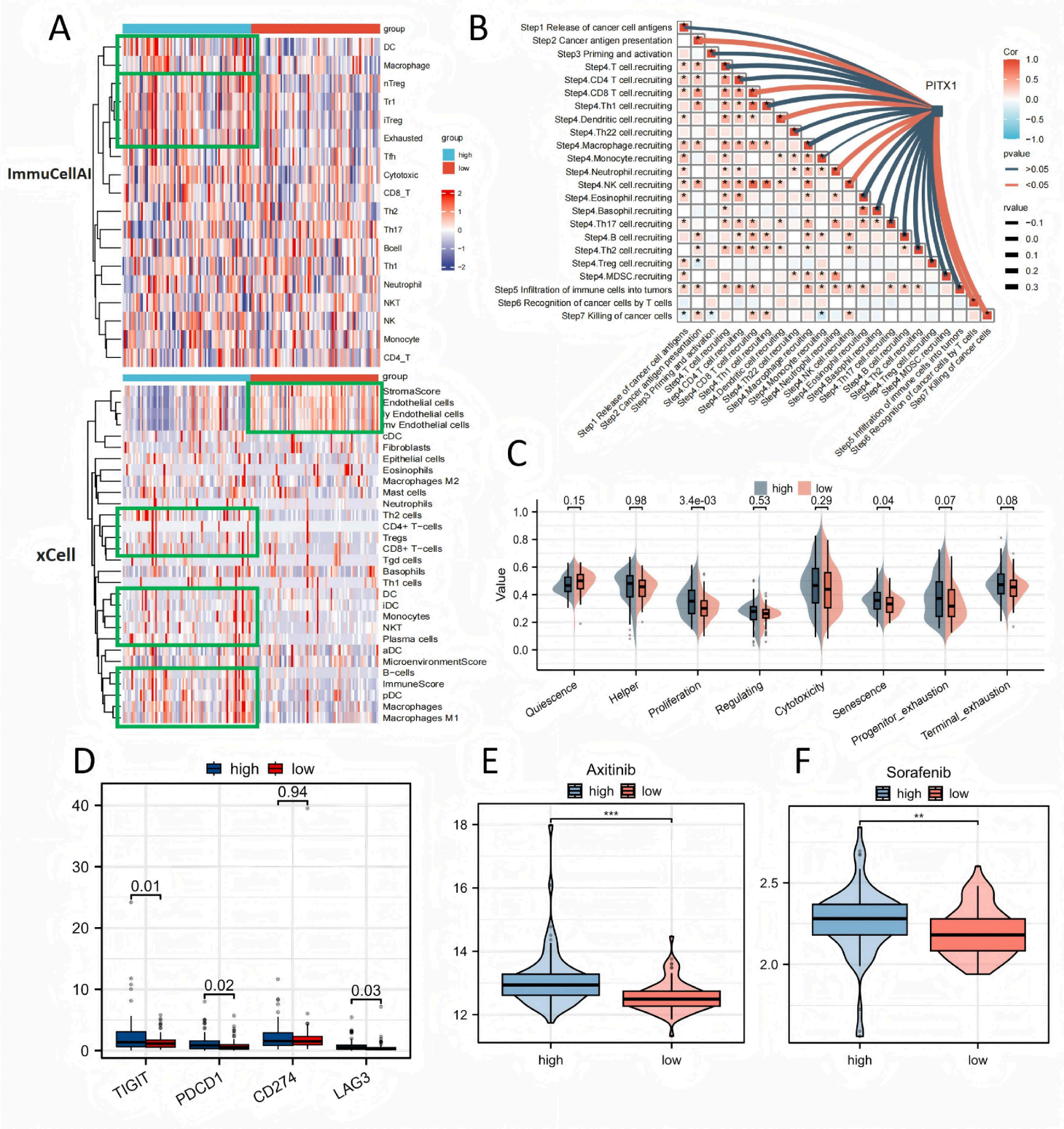


Figure 7

Immune-related analysis and drug sensitivity analysis. (A) Two algorithms, ImmuCellAI and xCell to perform immune cell infiltration analysis. **(B)** TIP divided the entire anti-cancer immune cycle into seven steps and tracked them. **(C)** “TCellSI” predicted the functional status of T cells and compared them in PITX1-high and PITX1-low groups. **(D)** Comparison of immune checkpoint expression at the mRNA level. **(E, F)** Drug sensitivity analysis was used to compare the IC50 value of axitinib and sorafenib between PITX1-high and PITX1-low groups. All the above analyses are based on the transcriptome matrix of WCH cohort. ImmuCellAI, Immune Cell Abundance Identifier; TIP, Tracking Tumor Immunophenotype; IC50, Half Maximal Inhibitory Concentration. *p<0.05, **p<0.01, ***p<0.001.

Supplementary Files

This is a list of supplementary files associated with this preprint. Click to download.

- SupplementaryFigure1.pdf
- SupplementaryTable1.docx
- SupplementaryTable2.xlsx